Structure of a dilute aqueous solution of argon. A Monte Carlo simulation

Giuliano Alagona and Alessandro Tani

Citation: The Journal of Chemical Physics **72**, 580 (1980); doi: 10.1063/1.438946
View online: http://dx.doi.org/10.1063/1.438946
View Table of Contents: http://scitation.aip.org/content/aip/journal/jcp/72/1?ver=pdfcov
Published by the AIP Publishing

Structure of a dilute aqueous solution of argon. A Monte Carlo simulation

Giuliano Alagona and Alessandro Tani[a)]

Laboratorio di Chimica Quantistica ed Energetica Molecolare del C.N.R., Via Risorgimento 35, 56100 Pisa, Italy

(Received 16 July 1979; accepted 20 September 1979)

A Monte Carlo simulation of a dilute aqueous solution of argon has been performed in the canonical (T,V,N) ensemble. The argon–water pair potential energy function has been obtained, with a best fitting procedure, from a set of 85 *ab initio* SCF energy values calculated with an extended basis set. Both energetic and structural evidences supporting the hypothesis of water structure promotion by nonpolar solutes are provided. Water molecules close to argon are oriented in a way similar to that of a crystalline clathrate cage. This analogy however is restricted to a local environment, which suggests that only parts of a real clathrate cage are present at a given time in this solution.

I. INTRODUCTION

In recent years, computer simulation methods such as molecular dynamics (MD)[1] and Monte Carlo (MC)[2] method, have provided an interesting approach to the problem of liquid state. Particularly for aqueous fluids, the classical theories of fluids are faced by overwhelming difficulties owing to their long-range, orientation-dependent, attractive intermolecular potential energy functions, while the various *ad hoc* models proposed give results which suffer the many drastic assumptions usually embodied in the partition function.[3]

Computer simulations, on the other hand, derive substantially exact values of mechanical quantities from a given potential energy function, which, in principle, can be improved at will. Thus, at present, their use is restricted only by practical problems, the greatest one being the large amount of computer time they require to deal with a number of particles representative of macroscopic systems. Their major inherent limit is actually that the computation of nonmechanical state functions, such as free energy and entropy, gives unreliable results, though some promising MC procedures are at present being developed to solve this problem.[4] Nevertheless, simulation methods have provided some of the most important recent advances concerning aqueous fluids.

Pure liquid water has been the subject of MD[5,6] and MC[7–13] calculations of increasing accuracy and, very recently, the aqueous solution of methane has also been MC simulated with results in good agreement with the experiments.[14,15] This particular system can be considered a simple model of the solution of nonpolar solutes in water. Much attention has been devoted[16] to the study of these solutions for two main reasons: (i) the role that water–solute interactions, present in this class of solutions, are considered to play to determine and maintain the three-dimensional structure of biological macromolecules in living cells, and (ii) the singular characteristics of these solutions as compared with those of the same solutes in other media.

The very low solubility of apolar solutes in water, for example, does not depend on the enthalpic term, that for the smallest solutes of this kind is negative, but on the larger decrease in entropy during the solution process. The latter feature, the entropy control of the solution thermodynamics, which is peculiar of aqueous solutions, has been used to classify this class of solutes as "typical aqueous."[16] Moreover, the decrease in entropy and the parallel increase in heat capacity, have to be ascribed, more than to the loss of rotational and translational degrees of freedom of the solute (they have been also observed in aqueous solutions of the rare gases), to variations of the structure of the solvent water induced by the solute. Many models have been developed to "explain" the thermodynamic results and the majority of them agrees on the hypothesis of Frank and Evans[17] that an apolar solute causes an increase in the order of neighboring water, producing what they called an "iceberg." This structure promotion effect could lead, according to certain authors,[18,19] to the formation of polyhedral cages of water molecules analogous to those of crystalline clathrate hydrate.[20] These qualitative pictures have received support from the simulations quoted above[14,15] which have shown that a water structure stabilization does really occur in the aqueous solutions of methane.

The purpose of this paper is, more than the reproduction of some thermodynamical quantities, the geometrical and energetical analysis of the dilute aqueous solution of argon to get information not available by other means. In particular, we have sought some evidence that could show that the clathrate cage model is preferable to the other ones or vice versa. Finally, the results we have reached could be used to contrast those of a similar study we plan to perform on an aqueous solution of a solute whose molecule both includes an apolar region and a polar group.

II. DETAILS OF CALCULATION

Our MC calculation has been performed in the canonical (T, V, N) ensemble according to the Metropolis scheme.[2] General principles and application techniques of Monte Carlo method have been reviewed by several authors.[21–25]

[a)] Postdoctoral fellow of the Scuola Normale Superiore di Pisa, Piazza dei Cavalieri, 56100 Pisa, Italy.

 0021-9606/80/010580-09$01.00

The system we have simulated is composed by one argon atom surrounded by 124 water molecules at 25 °C, with a volume equal to the sum of the experimental partial molar volumes of argon[26] and water, practically a cubic box with a side of 15.57 Å.

As starting configuration we have chosen the cubic ice I_c lattice with 125 molecules. One of them has then been removed to create the cavity which hosts the argon atom. If compared with a random configuration, the crystalline arrangement has the advantage of excluding overlaps of two or more molecules, hence it might allow faster equilibration of the system. The starting regular disposition has been later destroyed by performing 30 000 steps at high temperature. Finally, the system has been allowed to equilibrate at the temperature of the calculation. The latter process has required about 250 000 steps before starting to average over a Markov chain of more than 500 000 steps. During this process, a geometrical configuration of the system each 1000 has been stored on magnetic tape to perform further analyses. To by-pass, at least in part, the approximation due to the use of a small number of water molecules and to reduce to border effects, periodic boundary conditions, in the minimum image distance convention,[27] have been used, though these are better suited for pure liquids than for solutions. This is particularly true for liquids with orientation-dependent intermolecular potential as water. However, the good agreement between calculated and experimental structural quantities[11-13] has made this widespread technique reliable.

Under the hypothesis of pairwise additivity, the total potential energy of one solute molecule (argon) plus N water molecules has been written as follows:

$$U_{sw} = \bar{U}'_s + U'_w = \sum_{i=1}^{N} U'_{sw_i} + \sum_{i=1}^{N} \sum_{j>i}^{N} U'_{w_i w_j} , \qquad (1)$$

where $\bar{U}'_s$ is the direct solute-solvent contribution to the partial internal energy of the solute, (the bar indicates a molar quantity), and U'_w is the configurational energy of N solvent water molecules. These contributions to the total energy U_{sw} have been computed with analytical functions both derived from *ab initio* quantum-mechanical calculations.

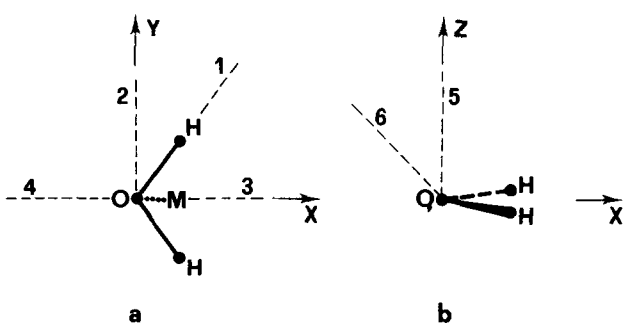

FIG. 1. The numbers indicate the various configurations of the complex Ar–H_2O in the planes XY (a) and XZ (b). The approach direction 7, not shown in figure, connects the origin with the $(-x, y, z)$ vertex of a cube, centered on the origin, whose quaternary axes are the Cartesian ones.

TABLE I. Coefficients of the argon–water intermolecular potential energy function.

Inverse power of r	O	H	M
1	$-0.682\,932\times10^{-1}$ [a]		
4			$0.476\,076\times10^{2}$ [b]
6	$-0.704\,474\times10^{3}$ [c]	$-0.247\,153\times10^{3}$ [c]	
12	$0.826\,476\times10^{6}$ [d]	$0.779\,255\times10^{5}$ [d]	$0.866\,077\times10^{6}$ [d]

[a] kcal Å/mole.
[b] kcal Å^4/mole.
[c] kcal Å^6/mole.
[d] kcal Å^{12}/mole.

III. INTERMOLECULAR POTENTIAL ENERGY FUNCTIONS

A. Argon–water

The argon–water intermolecular potential energy function has been obtained by best fitting an empirical function to the potential energy hypersurface of the complex H_2O–Ar, sampled with 85 *ab initio* self-consistent field (SCF) quantum mechanical energy values.[28] This set includes points with an Ar–O distance ranging from 3.3 to 7.7 Å, for seven different approach directions (see Fig. 1). The relevant interaction energies are between -0.087 and 0.25 kcal/mole.

For the sake of internal coherence and computational economy, we have used, in order to fit the argon–water potential, the same model of water molecule employed for fitting the configuration interaction (CI) water–water potential.[29] In this model (see Fig. 1), a water molecule is described by four points, three being the atomic nuclei, while the fourth, the M point, which bears the negative charge in the CI water potential, lies on the C_{2v} symmetry axis 0.2676 Å far from the oxygen. The molecular geometry, held fixed throughout the calculation, has the experimental values[30] of bond length and angle, 0.9572 Å and 104.52°, respectively.

As the potential energy between argon and the solvent water must be calculated at each step of the Markov chain, it is of great importance that the fitting function used for this computation is as fast as possible and, at the same time, accurate enough to get reliable results in the MC simulation. To this end, we have started from a linear combination of terms which can be written as follows:

$$V = \sum_{\alpha=1}^{4} \sum_{n=1}^{K} \alpha_{n\alpha} r_{\mathrm{Ar}\,\alpha}^{-n} , \qquad (2)$$

where the a's are adjustable parameters and the r's the distances between argon and each α point on the water molecule. We have tested, with a multiple linear regression program,[31] many functions of this class, varying the number of terms with a stepwise procedure. Table I shows the function which best balances the accuracy of fitting and computational speed, together with the optimized parameters. The standard error of the estimate of our fitting is 0.0085 kcal/mole and the multiple correlation coefficient squared, i.e., the part of the energy total variance accounted for by this model, is $R^2 = 0.9867$. The agreement between calculated and

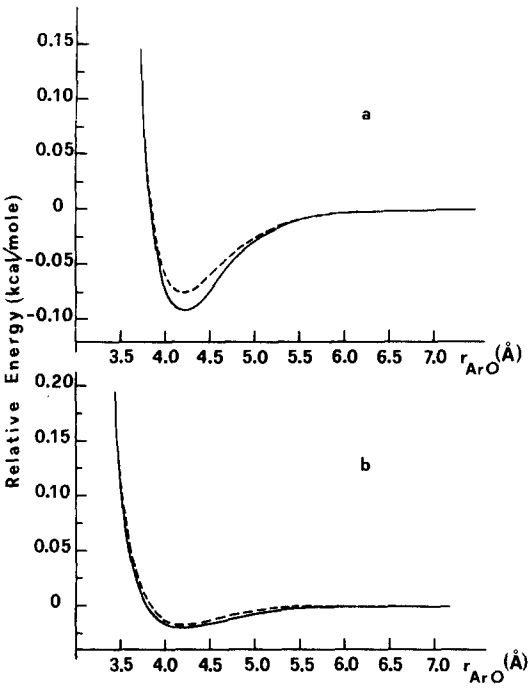

FIG. 2. Variation of the argon-water interaction energy with distance, with respect to the isolated species, for approach direction 1 (a) and 6 (b). Full lines: self-consistent field (SCF) calculated values, dashed lines: fitted values.

fitted values can be seen in Fig. 2(a) for direction 1, where the absolute minimum has been found, and in Fig. 2(b) for direction 6 (region of the lone pairs).

Though this function does not aim at being a physical description of the interactions between water and argon, it contains terms closely similar, even in the sign of their parameters, to those of the Lennard-Jones potential, while others should be given a mostly numerical character. The essentially repulsive nature of the argon–water potential compared with the water–water one (~ −0.1 kcal/mole against ~ −5.6 kcal/mole in their minima) did not justify, in our opinion, empirical corrections for the dispersion forces not accounted for by the Hartree–Fock method, or the additional computational effort required to improve it with CI calculations.

B. Water–water potential

The function we have used is the fitting function of Matsuoka *et al.*,[29] which was obtained after the most extensive CI calculations reported to date, for a large portion of the potential energy hypersurface of the water dimer. The same function has been also tested, with fairly good results, in MC simulations of pure liquid water[11–13] and dilute aqueous solution of methane.[14,15]

IV. RESULTS AND DISCUSSION

A. Energy calculations

As we are simulating a solution, our main interest is devoted to changes rather than to absolute values of mechanical properties of the system. For example, the partial molar internal energy of argon can be defined as

$$\bar{U}_s = U_{sw} - U_w \,, \tag{3}$$

where U_{sw} is expressed by (1) and U_w represents the potential energy of N water molecules in the pure liquid state. The standard we have chosen to compare our results for the aqueous solution of argon is the MC simulation of pure water performed by Swaminathan and Beveridge.[13] Their work has been carried out with the same values of N and T we have used and with a density value of water we have corrected for the inclusion of the argon atom. Moreover, the same water–water potential energy function and the minimum image convention for the periodic boundary conditions are used, with a Markov chain of comparable length.

Table II collects all the energetic results of our calculation. Unfortunately, the accuracy of the computed heat capacity makes the calculation of the relevant partial molar quantity not reliable. The value of $\bar{U}_s$ (−9.0 kcal/mole) we have obtained for argon is close to those found in MC simulations of the dilute aqueous solution of methane.[14,15] The same analogy can be found between the experimental thermodynamic properties of the relevant aqueous solutions, as it is shown in Table III, and we believe that this parallelism can be considered an evidence of the reliability of the calculated results.

As can be seen, the agreement between calculated (−19.0 kcal/mole) and observed (~ −3 kcal/mole, see Table III) partial molar internal energy of argon is only qualitative. The rather high error (~63%) on the value of the calculated $\bar{U}_s$ (see Table II) is typical of this kind of calculation,[14,15] but this is not surprising if one considers that we are seeking for the little difference between great and close numbers. The negative sign of the experimental quantity, however, is correctly reproduced by this simulation. Moreover, what is more important, if we define the relaxation energy

$$\bar{U}_{\rm rel} = U'_w - U_w \,, \tag{4}$$

as the difference between the energy of an equal number of moles of solvent (U'_w) and pure (U_w) water, we can decompose the partial molar internal energy of argon into two parts:

TABLE II. Calculated values of the internal energies for the aqueous solution of argon in kcal/mole.

U_{sw} ($N_w = 124$, $N_s = 1$)	−1072.9 ± 4.3[b]
U_w ($N_w = 124$)	−1063.9[a] ± 3.7[b]
U'_w ($N_w = 124$)	−1075.1 ± 4.3[b]
$\bar{U}'_s$	2.2 ± 0.85[b]
$\bar{U}_{\rm rel}$	−11.2 ± 5.7[c]
$\bar{U}_s$	−9.0 ± 5.7[c]

[a]Value taken from Ref. 13.
[b]The standard deviations are determined by averaging over partial chains of 25 000 steps, according to the method proposed by Wood (Ref. 22).
[c]The standard deviations of the calculated difference quantities are the square roots of the sums of the component variances.

TABLE III. Values of variations of some thermodynamic properties in water at 25 °C for argon and methane during the process: solute {ideal gas at $P = 1$ atm.} → solute {hypothetical ideal solution at unit mole fraction}.

	$\Delta C^0_{P,h}$ (cal/mole deg)	ΔH^0_h (kcal/mole)	ΔS^0_h (cal/mole deg)	ΔG^0_h (kcal/mole)	Ref.
Argon	42.6	−2.93	−30.9	6.27	32
	44.5	−2.86	−30.6	•••	33
	•••	−2.74	−30.2	6.26	36
	•••	−2.88	−30.7	•••	35
Methane	49.6	−3.30	−32.1	6.28	32
	55	•••	•••	•••	36
	•••	−3.05	−31.2	6.25	37
	•••	−3.19	−31.8	6.29	38,39

$$\bar{U}_s = \bar{U}'_s + \bar{U}_{rel} , \tag{5}$$

where $\bar{U}'_s$ is defined by (1) and $\bar{U}_{rel}$ accounts for the variation of the solvent water energy induced by the solute. This partitioning of the total value into a solute repulsive term ($\bar{U}'_s$) and a greater, attractive, solvent configurational term ($\bar{U}_{rel}$), supports the hypothesis that variations in the solvent water structure are responsible for the energetically favorable balance of this solvation process. The excessive value of $\bar{U}_{rel}$ (and hence of $\bar{U}_s$) could depend on several factors. First of all, in our opinion, it must be stressed that this model solution has a nonrealistic concentration value [1 Ar to each 124 H_2O versus an experimental solubility of ~1/40 000 (Ref. 40)], which does not allow the presence of as many unperturbed "bulk" water molecules as in the real solution, thus magnifying the solvent stabilization effect due to the argon atom. Second, it should be borne in mind that our calculation includes a number of approximations which can cause some error. One could wonder about how large are the effects due to neglecting the three- and many-body interactions in the water configurational energy as well as the electronic correlation in the Ar–H_2O potential energy. According to Lie *et al.* [11] the many-body terms should correct the internal energy of the pure liquid water by ~1 kcal/mole, but their importance could be different for the Ar–H_2O solution. Thus, they could contribute to the large value of $\bar{U}_s$, as already observed, [15] even if the error inherent to the pairwise approximation cancels out, to a certain extent, when taking the difference between the internal energy of the solution and of the pure liquid water. As for the electronic correlation neglected in the Ar–H_2O potential energies calculations, we believe that it should not affect the calculated $\bar{U}_s$ value in a noticeable way.

B. Argon–water radial distribution functions

Figures 3 and 4 show the argon–oxygen and argon–hydrogen radial distribution functions, (rdf), $g_{ArO}(r)$ and $g_{ArH}(r)$ respectively, together with the relevant running coordination numbers, $N_{ArO}(r)$ and $N_{ArH}(r)$. As one can see, in the $g_{ArO}(r)$ rdf there is a first solvation shell extended from 2.8 to 5.0 Å from the argon atom, which contains ≅ 17 water molecules (more precisely, the average coordination number for the oxygen atom is 16.84 and for the hydrogens 33.64).

A second broad shell is also present with the maximum 6.1 Å apart from Ar, so the distance between the first and second maximum of the curve, ~2.5 Å, lies in the range of separations typical of H bonds. The argon–hydrogen rdf has its first maximum only ~0.2 Å closer to argon than the $g_{ArO}(r)$, showing that, on the

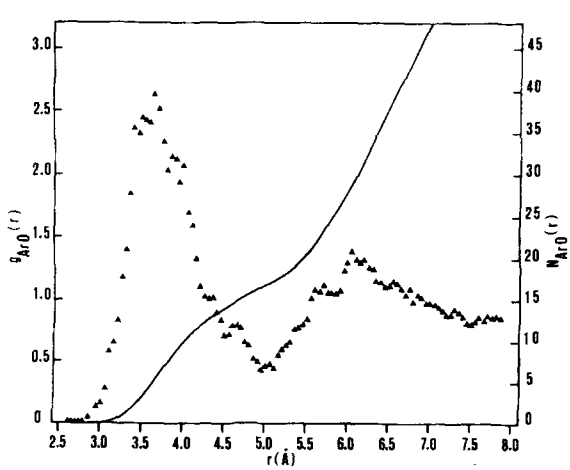

FIG. 3. Calculated argon–oxygen radial distribution function $g_{ArO}(r)$ (▲) and running coordination number $N_{ArO}(r)$ (full line).

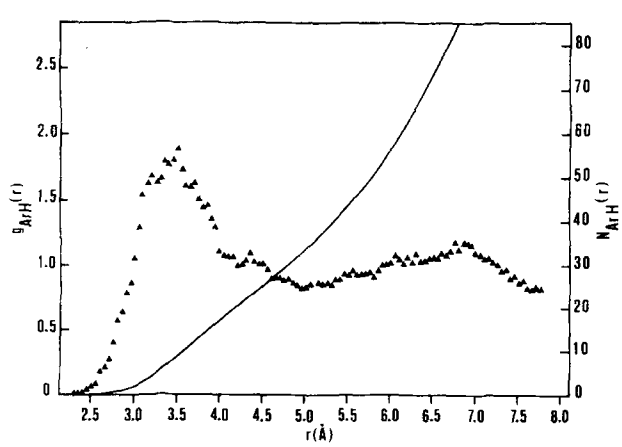

FIG. 4. Calculated argon–hydrogen radial distribution function $g_{ArH}(r)$ (▲) and running coordination number $N_{ArH}(r)$ (full line).

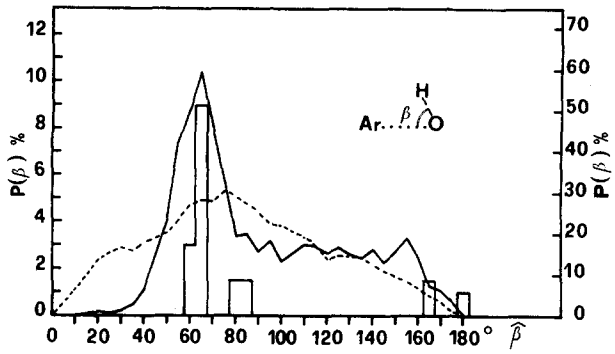

FIG. 5. Probability density function of the angles β formed by argon, an oxygen and each of the four hydrogens closest to it. The histograms relate to crystalline clathrate hydrate (right-hand scale). The full line curve relates to first shell molecules (i.e., with $r_{ArO} \leq 5$ Å) and the dashed line curve to bulk water ($r_{ArO} > 5$ Å).

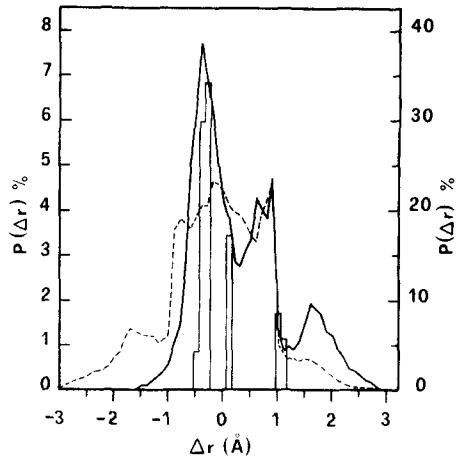

FIG. 7. Probability density function of the differences $\Delta r = r_{ArO} - r_{ArH}$, for each of the four hydrogens closest to an oxygen. The histograms relate to crystalline clathrate hydrate (right-hand scale). The full line refers to a first shell oxygen; the dashed line to a bulk one.

average, there is no hydrogen pointing radially inward. The values of the coordination numbers and the distance of the first maximum of $g_{ArO}(r)$ from argon (~3.6 Å) could be a first indication that the water molecules around the solute might be disposed in a structure somewhat resembling a clathrate cage.[20]

C. Orientational structure of the solvation shells

In order to reach a clearer insight into the microscopic structure of water surrounding the argon atom, we have calculated the set of probability density functions (pdf) (more correctly: percentage frequency) shown in Figs. 5–8. For each function results are reported for the molecules of the first hydration shell (i.e., with a distance between Ar and the O, taken as reference point, up to 5.0 Å), as well as for the outer ones. Where possible, the relevant data for the crystalline clathrate hydrate[41] are also given as histograms. The latter have been added to check if patterns typical of this structure are present in the first solvation shell and/or in the rest of the solution. Figure 5 shows the probability density function of the angles (ArÔH) formed by argon, an oxygen, and each of the four hydrogens closest to it, i.e., its two hydrogens plus two nearest-neighbor hydrogens belonging to other molecules.[42] We have chosen to include these "external" hydrogens in this analysis to better understand how argon sees the basic structural unit formed by a more or less distorted tetrahedron with an oxygen at its center and four hydrogens on the lines connecting the center with the vertices. From this figure the difference between the first shell and the rest of the solution stands out clearly. The distribution for the first shell is actually much more structured and remains practically zero up to ~35°, a range where the pdf values for the outer molecules are about half their maximum. This shows that orientations with a hydrogen pointing radially inward quite rarely appear in the first shell, while they occur with an high probability for larger distances from argon. Furthermore, it can be noted that the curve corresponding to the first shell reproduces much more closely the distinctive features of the clathrate cage, chiefly the maximum and the shoulder on its right. In the region of large angles the peak at ~155° is representative of the two little peaks at ~160° and 180° of the clathrate. This attribution can be verified more clearly in Fig. 6, where

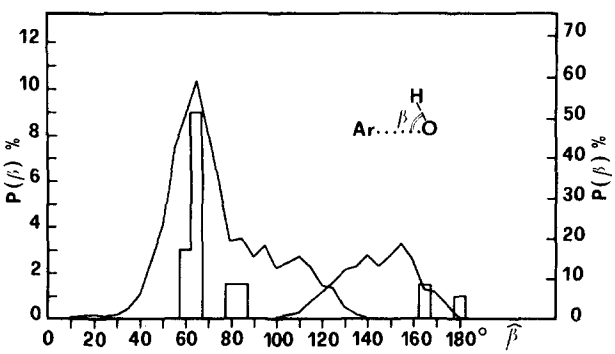

FIG. 6. Probability density function of the same angles β of Fig. 5, decomposed into the contribution of the hydrogen farthest from argon (right-most region of the curve) and of the other three hydrogens.

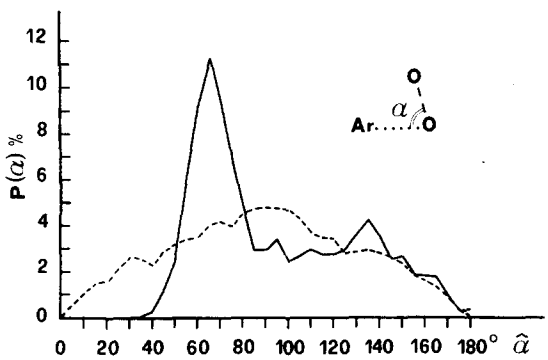

FIG. 8. Probability density function of the angles α formed by argon, an oxygen and each of the four oxygens closest to it. Full line relates to first shell molecules and dashed line to bulk water.

the distribution has been decomposed into the contributions of the hydrogen farthest from argon (peak on the right of the figure) and of the other three hydrogens. To explain, at least in part, the width and position of this right-most peak, it must be borne in mind that the model of water molecule derived from the CI potential is not a tetrahedral one. Actually the curve of potential energy of the dimer as a function of the rotation around an axis perpendicular to the lone pairs plane, shows a flat minimum, with almost constant values, over a range of ~80°, for distances O–O between 2.5 and 3.5 Å. This, in its turn, causes angles ArÔH ranging from 120° to 180° to be almost equally probable.

The orientation of water molecules with respect to argon can also be studied with an alternative approach, i.e., by examining the pdf of the difference $\Delta r = r_{ArO} - r_{ArH}$ (see Fig. 7), where r_{ArH} is the distance from argon of each of the same four hydrogens considered for the pdf of Fig. 5. Here again the curve for first shell molecules better reproduces the clathrate histograms than the one for outer (bulk) molecules. The highest peak ($\Delta r \simeq -0.4$ Å) is due to hydrogens that, as in the clathrate cage, lie on nearly the same spherical surface of the oxygen to which they relate. The other two peaks ($\Delta r \simeq 0.5$–0.9 Å and $\Delta r \simeq 1.6$ Å) both result from hydrogens external to the oxygen. The right-most one comes from hydrogens which belong to outer molecules engaged in hydrogen bonding with first shell water. Therefore, this analysis also confirms that, on the average, the disposition of the tetrahedral units does not differ much from the "umbrella" orientation with three bonds folding argon and the fourth pointing radially outward.

Figure 8 shows the probability density function of the angles (ArÔO) formed by argon, an oxygen and each of its four nearest-neighbor oxygens. As one can see, for first shell molecules, the first part of this curve (from 0° to ~100°) is very similar to the same region of Fig. 5. In particular, both functions reach their maximum values (10.4% and 11.3% for ArÔH and ArÔO angles, respectively) at 65° and then they lower to values of ~3% from 80° to ~110°. On the other hand, the right-most part of this curve ($\alpha > 110°$) shows significant differences with respect to the same region of Fig. 5. This is particularly true for the peak at ~135°, due to $ArÔ_iO_j$ angles with j oxygens beyond 5 Å from Ar, which most likely relates to the peak at ~155° of the pdf for ArÔH angles (Fig. 5). From the festures of these pdf's, hence, the indication can be drawn that, on the average, the deviation from the alignment of the atoms O, H, and O engaged in a H bond is negligible for bonds between first shell molecules, but it increases up to ~20° for bonds connecting shell with bulk molecules.

Therefore, the data collected so far seem to indicate that the presence of a nonpolar solute, such as argon, increases the degree of orientational ordering of the nearby water. It must be pointed out, however, that the pdf's we have calculated can give information only on the local environment of a water molecule, as formed by its four nearest neighbors. So, they can by no means tell us if, as in a real crystalline clathrate hydrate, a number of these structural units links up together to build the cage which hosts the solute.

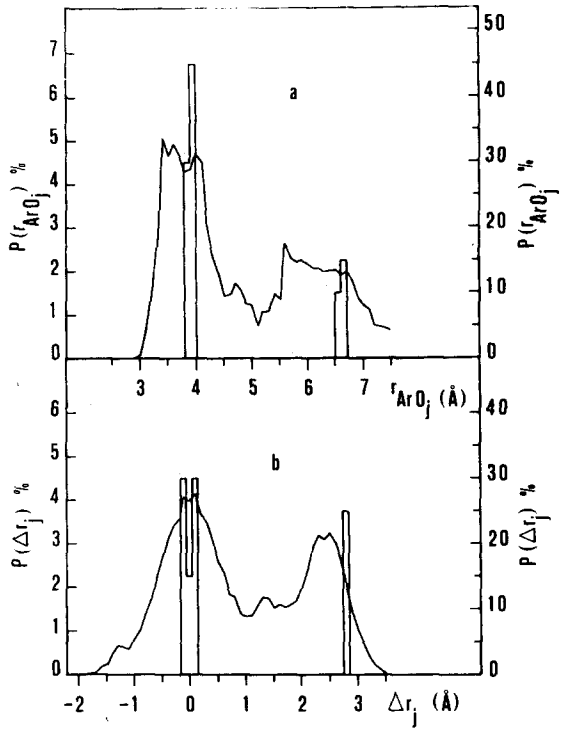

FIG. 9. (a) Probability density function of the distances r_{ArO_j} from argon of each of the four oxygens j nearest neighbor of an oxygen i of first shell. (b) Probability density function of differences $\Delta r_j = r_{ArO_i} - r_{ArO_j}$. In both parts of the figure the histograms relate to the crystalline clathrate hydrate (right-hand scales).

In order to clarify this point we have examined the behavior of solvent water molecules with the aid of the pdf's shown in Fig. 9. Figure 9(a) gives the probability density of the distances from argon of each of the four oxygens j closest to each oxygen i of the first shell (r_{ArO_j}). In Fig. 9(b) the distribution of the differences $\Delta r_j = r_{ArO_i} - r_{ArO_j}$ is reported. A comparison of these two curves shows that in Fig. 9(b): (a) we obtain a better definition of the peaks; (b) the position of their maxima can be determined much more accurately; (c) these maxima are very close to those of the relevant peaks of the clathrate.

As passing from (a) to (b) of Fig. 9 is the same as moving an observer from argon to an oxygen of the first shell, the above-mentioned differences suggest that at a local level the arrangement of four waters around a central one is almost regular (tetrahedral), but the degree of ordering greatly decreases if one considers first shell molecules as a whole. Actually Fig. 9(a) shows that argon sees the various tetrahedral units spread over a range of distances of more than 1 Å.

To summarize, then, the picture emerging from all the data collected is characterized by the presence, in the inner part of the solution, of tetrahedral units whose preferred orientation with respect to argon has a hydrogen, or a lone pair, pointing radially outward, just as in the clathrate cage. The latter, however, appears as a whole in the solution, if ever, in an extremely small fraction of the configurations examined.

V. WATER–WATER INTERACTIONS

A. Structure

The water–water interactions have been examined, from the structural point of view, through the oxygen–oxygen, oxygen–hydrogen, and hydrogen–hydrogen radial distribution functions, as well as through some parameters typical of hydrogen bonding.

Figures 10 and 11 show the $g_{OO}(r)$, $g_{OH}(r)$ and $g_{HH}(r)$ rdf's. The former figure matches the various rdf's for shell ($r_{ArO} \leq 5$ Å) and bulk water, while the latter compares the relevant functions for bulk and pure liquid water.[11] A comparison of these curves seems to suggest two major conclusions: (i) not so great differences appear between shell and bulk molecules; (ii) bulk water closely resembles pure liquid.

In particular the $g_{OO}(r)$ and $g_{OH}(r)$ for shell and bulk water never differ in a significant way except in the ranges 3.8–5.0 Å and 3.5–5.0 Å, respectively. The similarity of the first part of the curves indicates that a water molecule, as for its first coordination shell, does not feel the presence of the argon atom, i. e., it sees four water molecules arranged in the usual (tetrahedral) disposition, but this is not surprising if one considers that these functions depend only on the distance between pairs of atoms. As to the orientation of these tetrahedra with respect to argon, the curves exclude, consistently with what was previously shown, the possibility of bonds pointing radially inward. The latter arrangement, in fact, should reduce the height

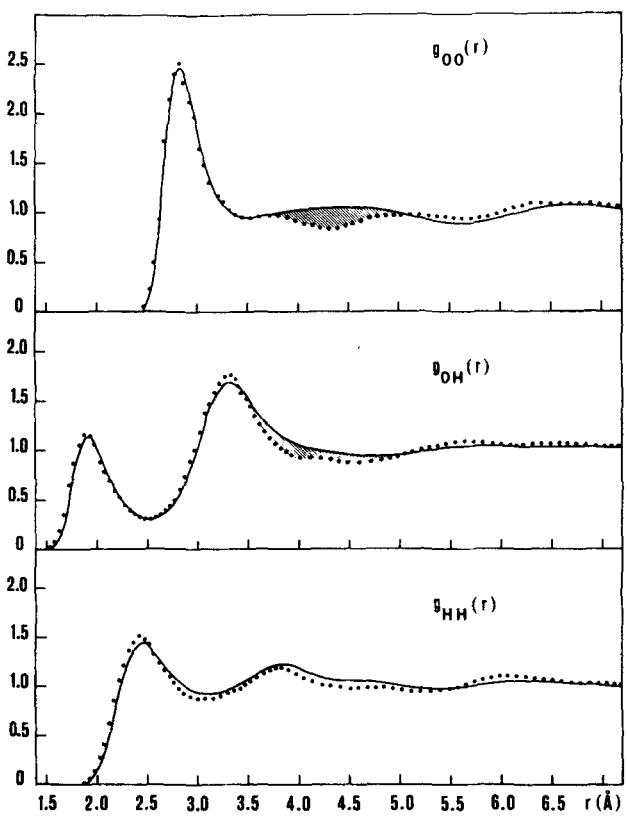

FIG. 10. Calculated radial distribution functions $g_{OO}(r)$, $g_{OH}(r)$ and $g_{HH}(r)$, for shell (dotted line) and bulk (full line) water.

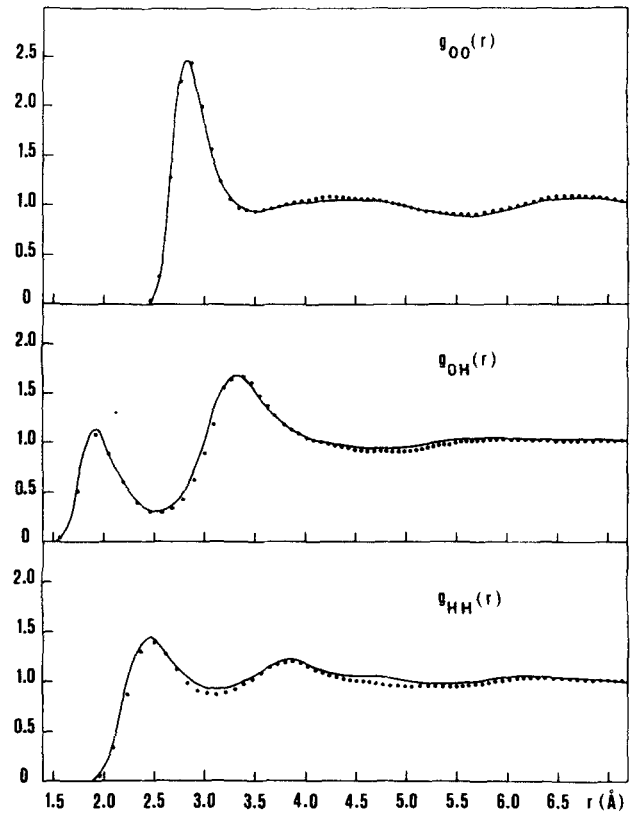

FIG 11. Comparison of calculated radial distribution functions for bulk (full line) and pure liquid water (dotted line). The data for pure liquid water are taken from Ref. 11.

of the first peaks of the shell rdf's, due to the substitution of a water molecule with the argon atom. The absence of this water molecule also causes the different behavior of shell and bulk curves in the shaded regions of Fig. 10. The difference of the coordination numbers between the limits mentioned above, is, in fact, 1.1 for the $g_{OO}(r)$ and 1.99 for the $g_{OH}(r)$ rdf. The above suggests that the geometrical features of the interactions between a pair of water molecules, as revealed by the radial distribution functions, are not very sensitive to their distance from argon or even to its presence. This holds true even if one considers the pdf of the angles $O\hat{O}H$ of the nearest-neighbor molecules (Fig. 12). The peak on the left in the figure indicates that the most probable deviation from the alignment in a H bond is ~15°, while that on the right shows the behavior of the same angle when oxygen j is a proton acceptor. The situation seems to change somewhat for the pdf of angles $O\hat{O}O$ inside the arrangement of a water molecule and the four ones closest to it (Fig. 13). It can be noted that, while the distribution for bulk molecules is unimodal with maximum at ~90°, that for shell molecules has two peaks with the most important one located near the value characteristic of a tetrahedral disposition.

B. Energetics

Structural variations induced by argon in the solvent water should be detectable, if present, also via the analysis of the values of interaction energy between

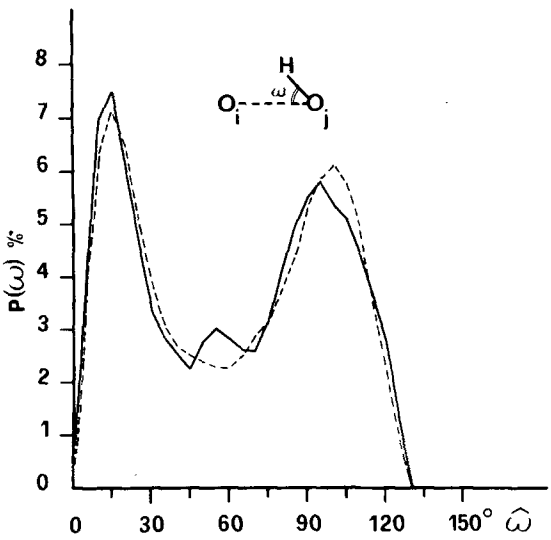

FIG. 12. Probability density function of the angle ω formed by the line joining oxygen i and j and the hydrogen, bonded with O_j, which is closest to O_i. Full line: shell molecules, dashed line: bulk molecules.

water molecules at different distances from the solute. Actually, the influence of the solute is revealed by the pdf of Fig. 14, where the probability density of the values of

$$U_i = \sum_{j=1}^{124} U_{ij} \quad (j \neq i) \tag{6}$$

is displayed for bulk and shell molecules. The curve relating to the latter molecules is on the whole a little shifted toward lower energies with a maximum slightly higher than for the bulk, consistent with what has been found by Owicki and Scheraga. [14]

These features are reflected by the mean values of the distributions, namely, $\langle U^s \rangle = -17.68$ kcal/mole and $\langle U^b \rangle = -17.26$ kcal/mole, with a difference $\Delta U = \langle U^s \rangle - \langle U^b \rangle = -0.42$ kcal/mole.

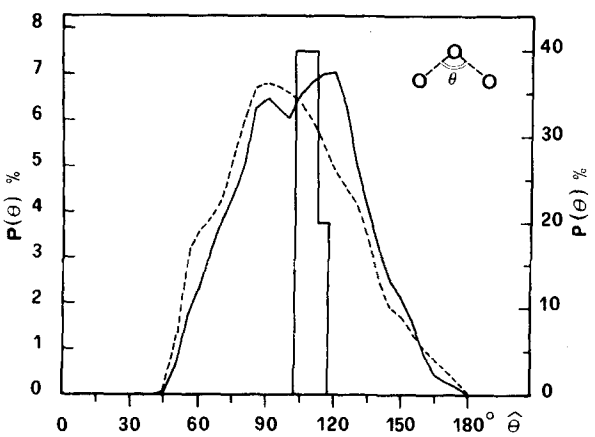

FIG. 13. Probability density function of the angle θ formed by sets of three molecules. The histogram relate to crystalline clathrate hydrate (right-hand scale). The curves refer to the solution. Full line: shell molecules, dashed line: bulk molecules.

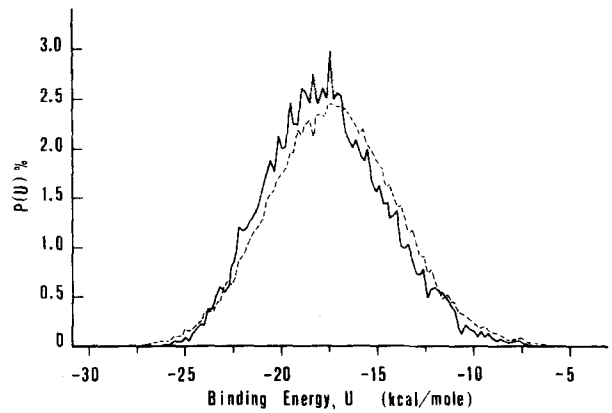

FIG. 14. Probability density function of the binding energy for a shell (full line) and a bulk (dashed line) water molecule.

A similar behavior is exhibited by the pdf for the interaction energy between the two nearest-neighbor (nn) water molecules (Fig. 15). In this case the mean value for shell molecules (both water molecules within 5.0 Å from Ar is $\langle U^s_{nn} \rangle = -3.57$ kcal/mole, while that for bulk molecules (both beyond 5.0 Å from Ar) is $\langle U^b_{nn} \rangle = -3.37$ kcal/mole. The difference turns out $\Delta U_{nn} = \langle U^s_{nn} \rangle - \langle U^b_{nn} \rangle = -0.2$ kcal/mole, which is about half the value of ΔU quoted above. The missing -0.22 kcal/mole are in part contributed by the other three molecules of the first coordination shell (cs) of each water molecule (see Fig. 16), whose mean values are $\langle U^s_{cs} \rangle = -3.00$ kcal/mole and $\langle U^b_{cs} \rangle = -2.98$ kcal/mole. To justify the rest of the difference (-0.16 kcal/mole), a little shift in the pair interaction energy at larger distance must be invoked, though some care must be taken on these arguments, owing to the little differences between these energy values.

VI. CONCLUSIONS

We have obtained results which support current ideas on the structure promoting effect of nonpolar solutes in water, and, perhaps, give them a more quantitative basis. The effects argon induces on nearby water are mainly orientational. It has been found that the tetrahedra centered on shell molecules are roughly oriented

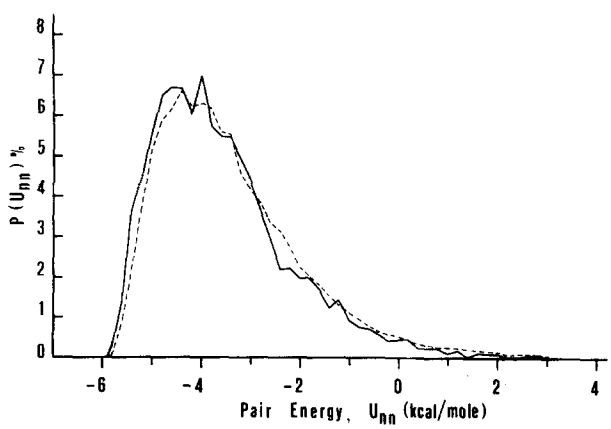

FIG. 15. Probability density function of pair interaction energy between nearest-neighbor shell (full line) and bulk (dashed line) water molecules.

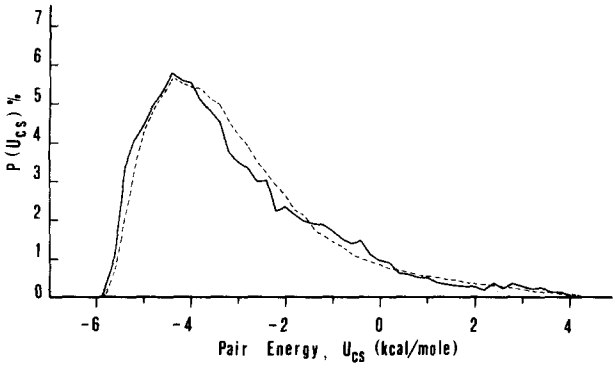

FIG. 16. Probability density function of pair interaction energy between a water molecule and three waters of its first coordination shell (cs). The fourth, the nearest neighbor, has been considered in Fig. 15. Full line: shell molecules, dashed line: bulk molecules.

as those of a clathrate cage. The latter, however, has not been observed as a whole in this simulation, though it seems to be very difficult to fix a limit that separates a set of water molecules from a distorted polyhedral cage.

A clear indication of enhanced structure is given by the lowering of pair interaction energies between a water molecule near the solute and its four nearest neighbors, as well as of its total binding energy. In this sense, interaction energy calculations have been revealed as a more powerful test to distinguish shell from bulk molecules, than, for instance, the various water–water radial distribution functions. Moreover, the loss of translational and rotational freedom, due to the excluded-volume effect of the inert solute, and the strengthening of pair interaction energy in nearby water, could explain, at least in part, the large decrease in entropy and increase in heat capacity experimentally observed in this class of solutions.

Finally, as to the limited numerical accuracy of our results, it must be borne in mind that it depends on the approximations at present required in the applications of Monte Carlo method, e. g., small number of molecules, neglect of many body effects and periodic boundary conditions. Nevertheless, we believe that these limitations do not seriously decrease the reliability of our conclusions.

ACKNOWLEDGMENTS

We would like to thank Professor Enrico Clementi and Dr. Silvano Romano for their useful suggestions. The stimulating discussions and critical reading of the manuscript by Professor Eolo Scrocco and Professor Jacopo Tomasi are gratefully acknowledged.

[1]B. J. Alder and T. E. Wainwright, J. Chem. Phys. **33**, 1439 (1960).
[2]N. Metropolis, A. W. Rosenbluth, M. N. Rosenbluth, A. H. Teller, and E. Teller, J. Chem. Phys. **21**, 1087 (1953).
[3]J. A. Barker and D. H. Henderson, Rev. Mod. Phys. **48**, 587 (1976).
[4]J. P. Valleau and G. M. Torrie, in *Statistical Mechanics, Part A: Equilibrium Techniques* (Vol. 5 of *Modern Theoretical Chemistry*), edited by B. J. Berne (Plenum, New York, 1977), Chap. 5.
[5]A. Rahman and F. H. Stillinger, J. Chem. Phys. **55**, 3336 (1971).
[6]F. H. Stillinger and A. Rahman, J. Chem. Phys. **60**, 1545 (1974).
[7]J. A. Barker and R. O. Watts, Chem. Phys. Lett. **3**, 144 (1969).
[8]H. Popkie, H. Kistenmacher, and E. Clementi, J. Chem. Phys. **59**, 1325 (1973).
[9]H. Kistenmacher, G. C. Lie, H. Popkie, and E. Clementi, J. Chem. Phys. **61**, 546 (1974).
[10]G. C. Lie and E. Clementi, J. Chem. Phys. **62**, 2195 (1975).
[11]G. C. Lie, E. Clementi, and M. Yoshimine, J. Chem. Phys. **64**, 2314 (1976).
[12]J. C. Owicki and H. A. Scheraga, J. Am. Chem. Soc. **99**, 7403 (1977).
[13]S. Swaminathan and D. L. Beveridge, J. Am. Chem. Soc. **99**, 8392 (1977).
[14]J. C. Owicki and H. A. Scheraga, J. Am. Chem. Soc. **99**, 7413 (1977).
[15]S. Swaminathan, S. W. Harrison, and D. L. Beveridge, J. Am. Chem. Soc. **100**, 5705 (1978).
[16]F. Franks, in *Water—A Comprehensive Treatise*, edited by F. Franks (Plenum, New York, 1973), Vol. 2, Chap. 5.
[17]H. S. Frank and M. W. Evans, J. Chem. Phys. **13**, 507 (1945).
[18]H. S. Frank and A. S. Quist, J. Chem. Phys. **34**, 604 (1961).
[19]D. N. Glew, J. Phys. Chem. **66**, 605 (1962).
[20]D. W. Davidson, in Ref. 16, Vol. 2, Chap. 3.
[21]J. M. Hammersley and D. C. Handscomb, *Monte Carlo Methods* (Methuen, London, 1964).
[22]W. W. Wood, in *Physics of Simple Liquids*, edited by H. N. V. Temperley, J. S. Rowlinson, and G. S. Rushbrooke (North-Holland, Amsterdam, 1968), Chap. 5.
[23]F. H. Ree, in *Physical Chemistry—An Advanced Treatise*, edited by H. Eyring, D. Henderson, and W. Jost (Academic, New York, 1971), Vol. VIII, Chap. 5.
[24]W. W. Wood, in *Fundamental Problems in Statistical Mechanics* III, edited by E. G. D. Cohen (North-Holland, Amsterdam, 1975).
[25]J. P. Valleau and S. G. Whittington, in Ref. 4, Chap. 4.
[26]E. W. Tiepel and K. E. Gubbins, J. Phys. Chem. **76**, 3044 (1972).
[27]W. W. Wood and F. R. Parker, J. Chem. Phys. **27**, 720 (1957).
[28]E. Clementi, private communication.
[29]O. Matsuoka, E. Clementi, and M. Yoshimine, J. Chem. Phys. **64**, 1351 (1976).
[30]W. S. Benedict, N. Gailar, and E. K. Plyler, J. Chem. Phys. **24**, 1139 (1956).
[31]*BMD—Biomedical Computer Programs*, edited by W. J. Dixon (University of California, Berkeley, 1971).
[32]E. Wilhelm, R. Battino, and R. J. Wilcock, Chem. Rev. **77**, 219 (1977).
[33]B. B. Benson and D. Krause, Jr., J. Chem. Phys. **64**, 689 (1976).
[34]S. Valentiner, Z. Phys. **42**, 253 (1927).
[35]D. M. Alexander, J. Phys. Chem. **63**, 994 (1959).
[36]L. A. D'Orazio and R. H. Wood, J. Phys. Chem. 67, 1435 (1963).
[37]W. F. Claussen and M. F. Polglase, J. Am. Chem. Soc. **74**, 4817 (1952).
[38]T. J. Morrison, J. Chem. Soc. 3814 (1952).
[39]T. J. Morrison and F. Billet, J. Chem. Soc. 3819 (1952).
[40]K. W. Miller and J. H. Hildebrand, J. Am. Chem. Soc. **90**, 3001 (1968).
[41]R. K. McMullan and G. A. Jeffrey, J. Chem. Phys. **42**, 2725 (1965).
[42]This minimum distance criterion has been checked by examining the various dimer configurations chosen with severe geometric and energetic tests, and the pdf's obtained this way closely reproduce those shown in this section.